

# Molecular Modeling of Stereo- and Regioselectivity of Group 4 Heterocenes in the Polymerization of Propene

Gaetano Guerra,<sup>†</sup> Paolo Corradini,<sup>‡</sup> and Luigi Cavallo<sup>\*,†</sup>

Dipartimento di Chimica, Università di Salerno, Via Allende, I-84081 Baronissi (SA), Italy, and  
Dipartimento di Chimica, Università di Napoli Federico II, Via Cintia, I-80126 Napoli, Italy

Received November 15, 2004; Revised Manuscript Received February 16, 2005

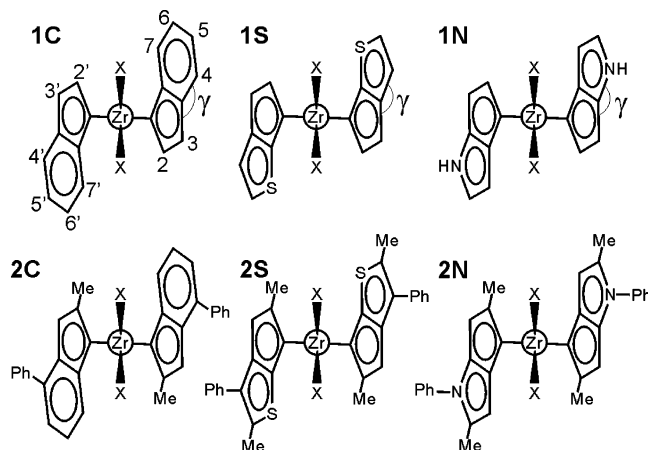
**ABSTRACT:** We report a theoretical analysis on the stereo- and regiochemical behavior of the S- and N-based group 4 heterocenes—developed by Ewen, Elder, and Jones—in the polymerization of propene to isotactic polypropylene. Somewhat surprisingly, the polymers produced with the N-based heterocene were shown to present a sensibly smaller amount of regiomistakes and a higher amount of stereomistakes relative to the S-based heterocene. To clarify the different mechanistic behavior of these structurally rather similar catalysts, we compared their stereo- and regioselectivity, and we extended our modeling to the corresponding all-carbon bis(indenyl)-based catalyst. Our analysis supports most of the ideas proposed by Ewen, Elder, and Jones to rationalize the experimental behavior.

## Introduction

Twenty years after the discovery that properly activated group 4 metallocenes such as **1C** and **2C** of Chart 1 are effective catalysts for the polymerization of 1-olefins,<sup>1,2</sup> the search for new catalysts still is an active field. Along the years, extensive and ingenious modifications of the parent systems were tested in order to achieve a control of the stereo- and regiospecificity, as well as of the molecular masses, of the produced polymers.<sup>3–6</sup> For example, different substituents were placed all over the basic bis(1-indenyl)-bridged skeleton of **1C**, and different bridges were inserted to link the two cyclopentadienyl (Cp) rings coordinated to the group 4 metal.<sup>3,4,6</sup> Recently, new synthetic paths considered the inclusion of heteroatoms in the basic metallocene skeleton.

In particular, Ewen, Elder, and Jones<sup>7</sup> (EEJ in the following) synthesized a new class of catalysts, named heterocenes, which contain a heteroatom in the ring fused to the bis(Cp) skeleton.<sup>8–10</sup> The obtained C<sub>2</sub>-symmetric heterocenes were proved very active in the polymerization of propene to isotactic polypropylene of high molecular masses.<sup>8</sup> However, the amount of stereo- and regiomistakes (SM and RM in the following) in the produced polymer is strongly dependent on the nature of the heteroatom of the catalyst. For the S-based heterocene **2S** of Chart 1 the amount of SM and RM is close to 0.41% and 0.35%, respectively.<sup>8</sup> These values are more or less comparable and consistent with the amount of SM and RM of the all C-based metallocene **2C** of Chart 1 (SM 0.19% and RM 0.49%).<sup>8</sup> However, in the case of the N-based heterocene **2N** of Chart 1 the amount of SM and RM is close to 1.43% and 0.10%, respectively.<sup>8</sup> These values indicate that **2N** is remarkably less stereoselective but more regioselective than both **2C** and **2S**, although the three systems substantially present the same substitution pattern. Because of the rather similar behavior of **2C** and **2S**, the different behavior of **2N** cannot be ascribed to the five-membered nature of the heterorings fused to the bis(Cp) skeleton in **2N**.

Chart 1



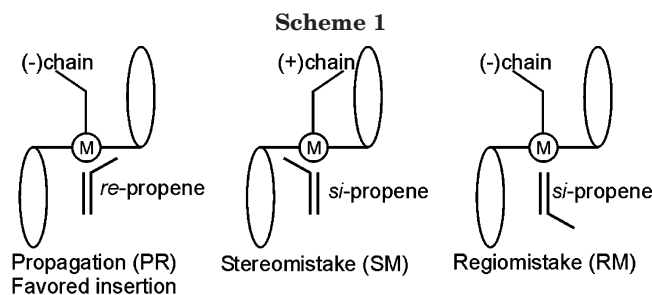
In this paper, we report on a theoretical analysis on the stereo- and regiochemical behavior of the systems **2C**, **2S**, and **2N**. To understand in detail the role of the Me and Ph substituents in positions 2,2' and 4,4', we also examined the simpler models **1C**, **1S**, and **1N** of Chart 1. In particular, we located the transition states for primary and secondary insertion of propene into the Zr–isobutyl bond of all the systems of Chart 1. As in our previous work, the isobutyl group simulates a primary growing chain. To determine the stereo- and regiospecificity of the systems of Chart 1, we investigated the structures schematically sketched in Scheme 1. Without loss of generality, all the calculations here reported refer to models with the (*R,R*) chirality of coordination of the aromatic ligand.

The structures in Scheme 1, left to right, correspond to the most favored transition state for propagation (PR in the following) and to the transition states leading to a SM and a RM. They are well accepted in the literature.<sup>3,4,6,11–13</sup> At this point, it is worthy to note that the same propene enantioface is involved in the transition states leading to a SM or a RM. For this reason, we define it the “wrong” enantioface. Consistently, we define “right” the propene enantioface that is involved in the most favored PR transition state. In the case of a *R,R* configuration of the catalyst, as in Chart 1 and

<sup>†</sup> Università di Salerno.

<sup>‡</sup> Università di Napoli Federico II.

\* Corresponding author. E-mail: lcavallo@unisa.it.



Scheme 1, the “right” and “wrong” propene enantiofaces are *re* and *si*, respectively. Within this framework, the stereoselectivity,  $\Delta E^+_{\text{stereo}}$ , is approximated as the energy difference between the transition states labeled SM and PR.<sup>14</sup> Consistently, and as commonly reported in the literature,<sup>15–19</sup> the regioselectivity,  $\Delta E^+_{\text{regio}}$ , is approximated as the energy difference between the transition states labeled RM and PR.<sup>14</sup> However, we recall that in a previous paper we proposed that a fine rationalization of RM in  $C_2$ -symmetric isospecific metallocenes (differently from  $C_s$ - and  $C_{2v}$ -symmetric syndio and aspecific metallocenes) can be better approximated as the difference between the activation energy for secondary insertion of the “wrong” monomer enantioface and the activation energy for coordination of the “right” enantioface ( $\Delta\Delta E^+_{\text{reg}}$  in eq 17 in ref 20). For this reason, we report also this other approximation to the regioselectivity,  $\Delta\Delta E^+_{\text{reg}}$ . Considering that the energy barrier for monomer coordination in structurally similar metallocenes can be reasonably estimated to be similar, we referred the regioselectivity of the systems of Chart 1 to the regioselectivity of the corresponding C-based system. Within this framework, the relative regioselectivity of **2N** is  $\Delta\Delta E^+_{\text{regio}} = \Delta\Delta E^+_{\text{reg}}(\mathbf{2N}) - \Delta\Delta E^+_{\text{reg}}(\mathbf{2C})$ . Finally, we remark that for  $C_2$ -symmetric and isospecific catalysts counterions have a minor role in stereo- and regioselectivity.<sup>6</sup>

### Computational Details

The Amsterdam Density Functional (ADF) program was used to obtain all the results discussed herein.<sup>21,22</sup> The electronic configuration of the molecular systems was described by a triple- $\zeta$  STO basis set on zirconium

for 4s, 4p, 4d, 5s, 5p (ADF basis set TZV).<sup>21</sup> Double- $\zeta$  STO basis sets, augmented by one polarization function, were used for S (3s, 3p), N and C (2s, 2p), and H (ADF basis sets DZVP).<sup>21</sup> The inner shells on zirconium (including 3d), sulfur (including 2p), nitrogen, and carbon (1s) were treated within the frozen core approximation. Energies and geometries were evaluated using the local exchange-correlation potential by Vosko et al.,<sup>23</sup> augmented in a self-consistent manner with Becke’s<sup>24</sup> exchange gradient correction and Perdew’s<sup>25,26</sup> correlation gradient correction.

Transition states were approached through a linear transit procedure. The distance between the two C atoms which form the new C–C bond was assumed as the reaction coordinate. Starting geometries were built using literature data<sup>27,28</sup> for the four-center Cossee-like transition state, and we started the scan on the assumed reaction coordinate from 2.5 Å downward, with a step size of 0.1 Å. At each point, the C–C distance assumed as the reaction coordinate was kept fixed while all the other degrees of freedom were fully optimized. Full transition state searches were started from the structures corresponding to the maximum of the energy along the linear transit paths. Convergence criteria in the geometry optimizations were set to  $1 \times 10^{-3}$  au on the maximum Cartesian gradient.

### Results and Discussion

All the four-center transition states we located assume a geometry consistent with the Cossee mechanism. Some of them are reported in Figure 1. In the most favored transition states **XX-PR** (**XX** = **1C**, **1N**, **1S**, **2C**, **2N**, **2S**) the growing chain assumes a (–) chiral orientation to minimize steric interactions with the *R,R*-coordinated ligand. In all these structures the *re* enantioface of the propene molecule reacts more favorably since it places the methyl group of the monomer away from (i.e., trans to) the growing chain. All these features are well consistent with the mechanism of the chiral orientation of the growing chain. In the transition states leading to a stereomistake, **XX-SM** (**XX** = **1C**, **1N**, **1S**, **2C**, **2N**, **2S**), the growing chain assumes a (+) chiral orientation. For the *R,R*-coordinated ligands of Figure 1 this orientation of the growing chain results in steric

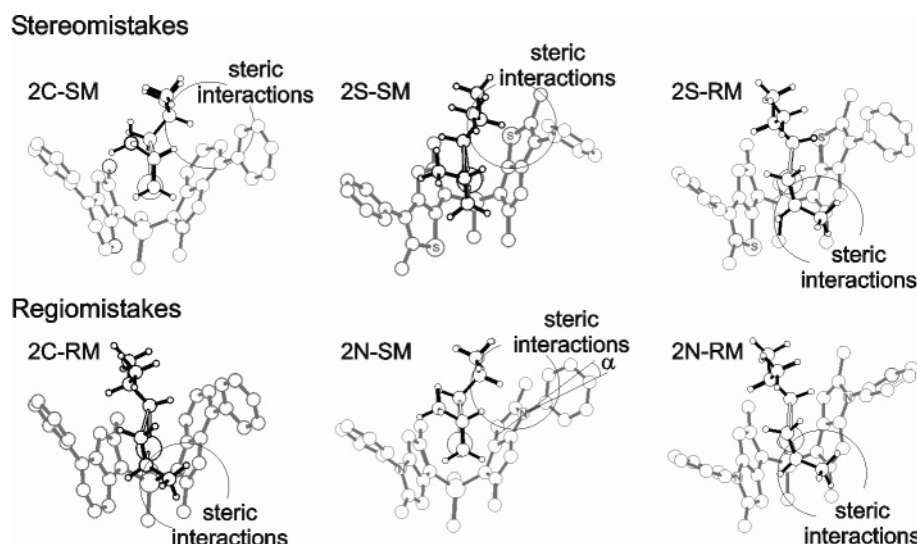


**Figure 1.** PR, SM, and RM transition states for systems **2C**, **2S**, and **2N**. The structure **2N-SM** is used to define the out-of-plane angle  $\alpha$ . The circles in the SM and RM structures indicate zones of steric interactions between the chain and the ligand (structures SM) or the monomer and the ligand (structures RM).

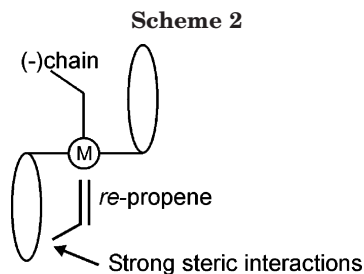


**Table 1. Energies (kcal/mol) and Most Relevant Geometric Parameters (Distances and Angles in Å and deg, Respectively) Relative to the Transition States Discussed in the Text**

	1C	1S	1N	2C	2S	2N
$\Delta E^+_{\text{stereo}}$	3.5	2.1	2.4	7.2	5.7	2.6
$\Delta E^+_{\text{regio}}$	3.5	3.4	3.1	3.9	3.8	4.6
$\Delta\Delta E^+_{\text{regio}}$	0	1.2	2.5	0	2.6	5.9
Zr–X <sub>Cp</sub> /OK <sup>a</sup>	2.26	2.25	2.25	2.27	2.26	2.25
Zr–X <sub>Cp</sub> /SM <sup>a</sup>	2.27	2.27	2.26	2.28	2.28	2.26
Zr–X <sub>Cp</sub> /RM <sup>a</sup>	2.26	2.26	2.25	2.27	2.27	2.26
X <sub>Cp</sub> ZrX <sub>Cp</sub> /OK <sup>b</sup>	127.4	127.9	127.2	128.3	127.9	128.6
X <sub>Cp</sub> ZrX <sub>Cp</sub> /SM <sup>b</sup>	127.0	127.7	127.6	127.1	127.7	128.2
X <sub>Cp</sub> ZrX <sub>Cp</sub> /RM <sup>b</sup>	127.1	127.2	127.4	127.7	127.2	128.4
$\alpha$ /OK <sup>c</sup>				2.8	3.0	9.3
$\alpha$ /SM <sup>c</sup>				0.8	1.8	8.5
$\alpha$ /RM <sup>c</sup>				2.6	3.3	12.4

<sup>a</sup> Mean Zr–X<sub>Cp</sub> distance in the PR, SM, and RM transition states (X<sub>Cp</sub> is the centroid of the Cp ring). <sup>b</sup> X<sub>Cp</sub>–Zr–X<sub>Cp</sub> angle in the PR, SM, and RM transition states. <sup>c</sup> Mean out-of-plane bending angle of the Ph substituent in the PR, SM, and RM transition states of **2C**, **2N**, and **2S**.

interactions with the ligand. Again, the methyl group of the monomer is oriented away from the growing chain.

As regards the transition states leading to a regiomistake, **XX-RM** (**XX** = **1C**, **1N**, **1S**, **2C**, **2N**, **2S**), the growing chain assumes the favored (–) chiral orientation, and the enantioface of the secondary inserting propene is the one that places the methyl group of the propene on the same side of the small Cp ring. This reduces steric interactions between the monomer and the ligand. Finally, we briefly remind that secondary insertion of the “right” enantioface is of very high energy, since the methyl group of the propene molecule is oriented toward the indenyl group (see Scheme 2). This theoretically explain<sup>15,29</sup> the high enantioselectivity observed experimentally in the occasional secondary insertion of propene with C<sub>2</sub>-symmetric metallocenes.<sup>30,31</sup> For this reason, secondary insertion of the “right” enantioface was not considered here.

The  $\Delta E^+_{\text{stereo}}$  reported in Table 1 clearly indicate that the unsubstituted **1C**, **1N**, and **1S** systems are not exceedingly enantioselective. However, the bis(1-indenyl)-based system **1C** is more enantioselective than the **1N** and **1S** heterocenes by roughly 1 kcal/mol. As pointed out by EEJ, closure of the five-membered heterocyclic ring requires larger  $\gamma$  angles (see Chart 1) relative to the all-C based ligand. In fact, the  $\gamma$  angle is close to 130° in **1C** and **2C**, while it is close to 140° in **1N**, **2N**, **1S**, and **2S**. They also reasoned that this geometrical feature pulls the N or the C4 atom of **1N** and **1S** away from the reactive pocket, reducing steric interactions with the growing chain. Our calculations support this idea.<sup>8</sup>

The presence of the Ph substituents in positions 4,4' of **2C** and **2S** increases the  $\Delta E^+_{\text{stereo}}$  of **2C** and **2S** by roughly 3 kcal/mol relative to **1C** and **1S**. In agreement

with the experimental results, this corresponds to remarkable stereospecific behavior.<sup>32,33</sup> Differently, the presence of the Ph substituent in **2N** results in a negligible increase of  $\Delta E^+_{\text{stereo}}$  compared to that of **1N**. The low  $\Delta E^+_{\text{stereo}}$  we calculated for **2N** again is in reasonable agreement with the experimental results. Examination of the geometrical parameters reported in Table 1 holds an explanation for this peculiar behavior. First, we note that the geometry of coordination of both the **2N** and **2S** heterocenes is rather similar to that of **2C**, as indicated by the substantially similar Zr–X<sub>Cp</sub> distances and X<sub>Cp</sub>–Zr–X<sub>Cp</sub> angles (X<sub>Cp</sub> = centroid of the Cp ring). Moreover, these basic geometric parameters are substantially similar in the PR transition states as well as in those leading to a SM or a RM. Conversely, the out-of-plane bending angle  $\alpha$  of the Ph substituents (see Figure 1) is remarkably different in **2C** and **2S** relative to **2N**. In the former systems, the C–Ph bond is substantially in the plane, with deviations smaller than 3–4° at most. In the **2N** systems, instead, the out-of-plane bending angle  $\alpha$  of the Ph groups is close to 9°. This implies that the partial sp<sup>3</sup> hybridization of the N atoms in **2N** pulls the Ph groups away from the reactive pocket, thus minimizing their role in determining a preferential chiral orientation of the growing chain and, consequently, the enantioselectivity of propene insertion. Thus, our analysis confirms the additional hypothesis proposed by EEJ to rationalize the poor stereospecificity observed in propene polymerization with the catalyst systems based on **2N**.<sup>9</sup>

As regards the regiochemistry of monomer insertion, the three unsubstituted **1C**, **1N**, and **1S** systems present more or less similar  $\Delta E^+_{\text{regio}}$ . This is reasonable since in all cases secondary propene insertion is disfavored by steric interactions between the methyl group of the monomer and the nearby Cp ring. In this respect, the three transition states present rather similar geometries/interactions around the methyl group of the secondary inserting propene (compare **1C-RM**, **1N-RM**, and **1S-RM** of Figure 1). Inclusion of the additional methyl group in positions 2,2' of the ligand increases the  $\Delta E^+_{\text{regio}}$  by roughly 1.0–1.5 kcal/mol. The increased regiospecificity in the presence of the additional methyl groups on the ligand is well known, and it is a clear consequence of direct steric interactions between the methyl group of the monomer and the methyl groups of the ligands, which are at short distance.<sup>13,16,33,34</sup> As regards, the Ph-substituted **2X** systems, we note that the  $\Delta E^+_{\text{regio}}$  of **2N** is remarkably greater than that of **2C** and **2S**, which are instead rather similar to each other. This is in good qualitative agreement with the experimental results, which clearly indicated that regioselectivity of the three systems is **2C** < **2S** < **2N**, although this approximation to regiochemistry is unable to capture the small difference between **2C** and **2S**.<sup>8</sup> As regards the other approximation to the regiochemistry of monomer insertion reported in Table 1,  $\Delta\Delta E^+_{\text{regio}}$ , the three substituted systems **2C**, **2S**, and **2N** present  $\Delta\Delta E^+_{\text{regio}}$  that increase sharply in the order **2C** < **2S** < **2N**. Thus, also the  $\Delta\Delta E^+_{\text{regio}}$  approximation we calculated is in reasonably good agreement with the experimental results, although this approximation exaggerates the difference between **2C** and **2S**.<sup>8</sup>

## Conclusions

In conclusion, in the present paper we investigated the stereo- and regiospecificity of some of the het-



erocenes catalysts proposed by EEJ. Our molecular modeling analysis clearly supports most of the ideas they proposed to rationalize the peculiar stereo- and regiospecific behavior of these systems, which is influenced by several interlaced factors. (i) The different size of the ring fused on the basic bis(Cp) skeleton imposes larger  $\gamma$  angles, which correspond to less crowded reactive pockets. (ii) The partial  $sp^3$  hybridization of the N atoms allows for an easy out-of-plane bending of the substituents bonded to them, thus reducing the values of  $\Delta E^+_{\text{stereo}}$ .

**Acknowledgment.** This work was supported by the MURST of Italy (Grants PRIN 2004 and FISIR 1999), by the University of Salerno (Finanziamento Piccole Apparecchiature 2002), and by Basell Polyolefins. We thank one of the reviewers for useful comments.

**Supporting Information Available:** Cartesian coordinates of all the structures discussed. This material is available free of charge via the Internet at <http://pubs.acs.org>.

## References and Notes

- Ewen, J. A. *J. Am. Chem. Soc.* **1984**, *106*, 6355.
- Kaminsky, W.; Külper, K.; Brintzinger, H. H.; Wild, F. R. W. P. *Angew. Chem., Int. Ed. Engl.* **1985**, *24*, 507.
- Brintzinger, H. H.; Fischer, D.; Mülhaupt, R.; Rieger, B.; Waymouth, R. M. *Angew. Chem., Int. Ed. Engl.* **1995**, *34*, 1143.
- Coates, G. W. *Chem. Rev.* **2000**, *100*, 1223.
- Corradini, L.; Cavallo, L.; Guerra, G. In *Metallocene Based Polyolefins, Preparation, Properties and Technology*; Scheirs, J., Kaminsky, W., Eds.; John Wiley & Sons: New York, 2000; Vol. 2, p 3.
- Resconi, L.; Cavallo, L.; Fait, A.; Piemontesi, F. *Chem. Rev.* **2000**, *100*, 1253.
- Elder, M. J.; Jones, R. L. Basell Polyolefins.
- Ewen, J. A.; Elder, M. J.; Jones, R. L.; Rheingold, A. L.; Liable-Sands, L. M.; Sommer, R. D. *J. Am. Chem. Soc.* **2001**, *123*, 4763.
- Ewen, J. A.; Elder, M. J.; Jones, R. L.; Rheingold, A. L.; Liable-Sands, L. M.; Sommer, R. D. *J. Am. Chem. Soc.* **2001**, *123*, 6964.
- Ewen, J. A.; Jones, R. L.; Elder, M. J. In *Metallorganic Catalysts for Synthesis and Polymerization*; Kaminsky, W., Ed.; Springer: Berlin, 1999; p 150.
- Busico, V.; Cipullo, R. *Prog. Polym. Sci.* **2001**, *26*, 443.
- Corradini, P.; Guerra, G.; Cavallo, L. *Acc. Chem. Res.* **2004**, *37*, 231.
- Guerra, G.; Cavallo, L.; Corradini, P. *Top. Stereochem.* **2003**, *24*, 1.
- A description of the elements of chirality and of the nomenclature used can be found in ref 12.
- Guerra, G.; Cavallo, L.; Moscardi, G.; Vacatello, M.; Corradini, P. *J. Am. Chem. Soc.* **1994**, *116*, 2988.
- Toto, M.; Cavallo, L.; Corradini, P.; Guerra, G.; Resconi, L. *Macromolecules* **1998**, *31*, 3431.
- Carbo, J. J.; Maseras, F.; Bo, C.; van Leeuwen, P. W. N. M. *J. Am. Chem. Soc.* **2001**, *123*, 7630.
- Borrelli, M.; Busico, V.; Cipullo, R.; Ronca, S.; Budzelaar, P. H. M. *Macromolecules* **2002**, *35*, 2835.
- Deubel, D. V.; Ziegler, T. *Organometallics* **2002**, *21*, 4432.
- Guerra, G.; Cavallo, L.; Corradini, P.; Longo, P.; Resconi, L. *J. Am. Chem. Soc.* **1997**, *119*, 4394.
- ADF 2004, Users Manual, Vrije Universiteit, Amsterdam, The Netherlands.
- te Velde, G.; Bickelhaupt, F. M.; Baerends, E. J.; Fonseca Guerra, C.; Van Gisbergen, S. J. A.; Snijders, J. G.; Ziegler, T. *J. Comput. Chem.* **2001**, *22*, 931.
- Vosko, S. H.; Wilk, L.; Nusair, M. *Can. J. Phys.* **1980**, *58*, 1200.
- Becke, A. *Phys. Rev. A* **1988**, *38*, 3098.
- Perdew, J. P. *Phys. Rev. B* **1986**, *33*, 8822.
- Perdew, J. P. *Phys. Rev. B* **1986**, *34*, 7406.
- Lohrenz, J. C. W.; Woo, T. K.; Ziegler, T. *J. Am. Chem. Soc.* **1995**, *117*, 12793.
- Cavallo, L.; Guerra, G. *Macromolecules* **1996**, *29*, 2729.
- Corradini, P.; Guerra, G.; Vacatello, M.; Villani, V. *Gazz. Chim. Ital.* **1998**, *118*, 173.
- Grassi, A.; Zambelli, A.; Resconi, L.; Albizzati, E.; Mazzocchi, R. *Macromolecules* **1988**, *21*, 617.
- Cheng, H. N.; Ewen, J. A. *Makromol. Chem.* **1989**, *190*, 1931.
- Spaleck, W.; Küber, F.; Winter, A.; Rohrmann, J.; Bachmann, B.; Antberg, M.; Dolle, V.; Paulus, E. *Organometallics* **1994**, *13*, 954.
- Stehling, U.; Diebold, J.; Kirsten, R.; Röhl, W.; Brintzinger, H. H.; Jüngling, S.; Mülhaupt, R.; Langhauser, F. *Organometallics* **1994**, *13*, 964.
- Röhl, W.; Brintzinger, H. H.; Rieger, B.; Zolk, R. *Angew. Chem., Int. Ed. Engl.* **1990**, *29*, 279.

MA047651Q